

Online supplement for:

Angiotensin-1 alters microvascular permeability coefficients *in vivo* via modification of endothelial glycocalyx

Andrew H.J. Salmon^{1,2}, Christopher R. Neal¹, Leslie Sage¹, Catherine A. Glass¹, Steven J. Harper¹, David O. Bates¹

Supplementary methods

Systemic microvessel permeability coefficient measurement

Experiments (as previously described¹) were performed on adult male *Rana temporaria* (obtained from Charles Sullivan, TN, USA) and on adult male Wistar rats (Harlan, UK). At the end of experiments, animals were sacrificed humanely by cranial destruction (frogs) or cervical dislocation (rats) while still under anaesthesia. All chemicals (as previously described¹) were obtained from VWR (Leics, UK) unless otherwise stated.

Frogs were anaesthetised by immersion in 1 mg.ml⁻¹ 3-aminobenzoic acid ethyl ester (MS222; Sigma, MO, USA) dissolved in tap water, then laid supine on an experimental stage. A 1cm vertical incision was made in the right flank, and the mesentery teased over a quartz pillar. Anaesthesia was maintained by continuously superfusing the mesentery with frog Ringer supplemented with 0.25 mg.ml⁻¹ MS222 throughout the experiment. Experiments were monitored in real time, and simultaneously videotaped for off-line analysis, as previously described¹. All experiments were performed at room temperature (20-22°C).

Capillary or post-capillary venular microvessels chosen for study were straight, at least 800µm in length, and free of side-branches and adherent leucocytes. Vessels were cannulated with a bevelled glass pipette, ground in-house from pulled glass capillary tubes (Clark Electromedical Instruments, Reading, UK). Hydrostatic pressure was applied to the lumen of the micropipettes via a water-filled manometer. Micropipettes were filled with Bovine Serum Albumin (BSA) (A4378 Sigma, MO, USA) dissolved in frog Ringer, using a syringe-driver / refiller system¹. Rat erythrocytes were added to the BSA solution at a concentration of 30µl.ml⁻¹, and acted as flow markers. Erythrocytes were collected by direct cardiac puncture of halothane-anaesthetised rats (5% halothane; Merial, Essex, UK), and washed at least three times in frog Ringer solution before use. Vessels were occluded up to 1400µm from the cannulation site by gently adjusting a micromanipulator (Prior, Cambridge,

UK and Stoelting, IL, USA) to lower the arm of a bent glass micro-occluder onto the vessel wall: the occlusion site was changed regularly and empirically.

Examination of microvascular permeability in rats was performed as above, with the following exceptions: anaesthesia was induced with 5% halothane (Merial, Essex, UK); maintenance of anaesthesia, physiological solutions used, and the experimental set-up were as described by our laboratory².

To determine the effect of Ang1 on L_p , BSA was supplemented with 200 ng.ml⁻¹ recombinant human Ang1 (rhAng1; R&D systems, MN, USA) (a concentration approximating the K_D 50 for Tie2-binding of Ang1, and previously shown to alter endothelial cell monolayer permeability *in vitro*³ and macromolecular leak *ex vivo*⁴). For pronase experiments, pronase (Sigma type XIV, P5147; added to 10mg.ml⁻¹ BSA at a final concentration of 0.1 mg.ml⁻¹). was introduced to the vessel for between 60 and 90sec, followed by resumption of perfusion with the initial solution (either 10mg.ml⁻¹ BSA alone, or 10mg.ml⁻¹ BSA supplemented with 200 ng.ml⁻¹ rhAng1). L_p was then measured during the ensuing 30 minutes. To examine whether Ang1 modifies L_p by translocating pre-formed substances from Golgi apparatus to the cell surface, vessels were co-perfused with Ang1 (200 ng.ml⁻¹) and the Golgi vesicle translocation inhibitor brefeldin A (100 μ m)⁵.

In all experiments, vessels were freely perfused with BSA-Ringer solution for 20 minutes following cannulation. Subsequent occlusion of the vessel resulted in steady movement of marker erythrocytes towards the occluder, indicating fluid efflux across the microvessel wall. Off-line examination of the rate of erythrocyte movement (dl/dt) in a vessel of known radius (r) and length (l) permitted determination of the rate of fluid efflux per unit area (J_v/A) using the equation

$$J_v/A = (dl/dt).(r/2l) \quad \text{(equation I)}$$

L_p was calculated using equation 1 (main report), assuming the luminal hydrostatic pressure to be equal to that in the manometer, the luminal oncotic pressure of 10 mg.ml⁻¹ BSA of 3.6 cmH₂O¹, and interstitial hydrostatic and oncotic pressures were assumed to be zero^{6,7}.

For determination of L_p alone, vessels were perfused with 10 mg.ml⁻¹ BSA. For determination of reflection coefficient for albumin (σ), vessels were perfused with 30 mg.ml⁻¹ BSA: identical results were observed with both solutions. For determination of σ , vessels were occluded at varying hydrostatic pressure. The rate of fluid efflux during each occlusion (calculated as above) was plotted against the imposed luminal hydrostatic pressure, and a linear regression line applied to the data points. The slope of the line describes L_p , and the abscissal intercept describes the measured mean effective oncotic pressure ($\sigma\Delta\pi$) of the luminal solution. Under the conditions of high J_v predicted with these experimental conditions, this latter term approximates to $\sigma^2\pi_c$ (e.g.⁸), permitting estimation of measured mean σ .

Electron microscopy of pronase-perfused microvessels

Frog microvessels were cannulated and perfused with either 10mg.ml⁻¹ BSA alone or 10mg.ml⁻¹ BSA supplemented with 200 ng.ml⁻¹ rhAng1 for 30 minutes, followed by exposure to pronase for <90sec, as described above. Following brief and transient perfusion with pronase, microvessels were immediately perfused with albumin-free Ringer solution for 1 min, followed by Alcian Blue solution for 5 min. Preparation of vessels for electron microscopy was then performed as described in the text. L_p measurement and electron microscopy were performed on separate populations of vessels for technical reasons, and because the aims of our study did not necessitate a quantitative comparison between changes

in the depth of endothelial glycocalyx (as revealed by electron microscopy) and permeability coefficient magnitude.

Glomerular permeability coefficient measurement

Rats were anaesthetised with 5% halothane (Merial, Essex, UK), and killed by cervical dislocation. Laparotomy and bilateral nephrectomy were performed immediately post-mortem, and kidneys placed in mammalian Ringer solution containing 10 mg.ml⁻¹ BSA (A7906 Sigma, MO, USA), as previously described⁹. The outer 1-2mm of superficial renal cortex was dissected from both kidneys, and glomeruli isolated using a standard sieving technique¹⁰ were transferred to either control or test solution at 37°C. Glomeruli that were free of Bowman's capsule and arteriolar or tubular fragments, and macroscopically intact, were chosen for study. All glomerular observations were performed within 3 hours of nephrectomy.

Micropipettes were pulled from glass capillary tubes (o.d. 1.2mm; Clark Electromedical Instruments, Reading, UK), and the 15µm aperture tip placed within a flange-ended, rectangular cross-section glass microslide (i.d. 400µm x 4mm; Camlab, Cambridge, UK) above the microscope and associated equipment (described above). Perifusate (containing mammalian Ringer and either 10 mg.ml⁻¹ ("dilute perifusate") or 80 mg.ml⁻¹ ("concentrated perifusate") BSA) was held in one of two heated glass reservoirs (Radnoti, CA USA) above the microslide, connected to the microslide via a series of heat-insulated Tygon tubes (Fisher, UK), which passed through either channel of an either/or rapid-response remote tap (Bio-Chem Valve Inc. 075P3), placed as close as possible to the micropipette tip. The reservoirs and tubing were heat-regulated to achieve a flowing perifusate temperature (at the locus of the glomerulus) of 37±0.5°C in all experiments. Flow rates (typically 1ml.s⁻¹) for each perifusate were calculated and equalised before introduction of glomeruli.

After a 2min period of equilibration, “dilute” perfusate was rapidly changed to “concentrated” perfusate, resulting in Schlieren lines around the glomerulus. Perifusate switches were recorded on video tape at 50 fields per second. Video sequences were reviewed (off-line). The glomerular outline was traced electronically (Adobe Systems Inc., CA, USA), and the area (A ; μm^2) of the glomerular image calculated using Image J (US National Institutes of Health) by assuming sphericity. Glomerular volume was plotted against time since first appearance of the Schlieren phenomenon, and two regression lines were applied to these points. The slope of the first line was prescribed as zero, and this first line was applied to points covering the period before perfusate switch, when baseline glomerular volume was stable. The second line was applied to points between 0.04s and 0.1s after perfusate switch: within these confines, the points to which an applied regression line had the greatest slope were chosen. The slope of the second regression line describes the greatest initial rate of change of glomerular volume; this equates with the term J_V in Starling’s equation. Hydrostatic forces across the isolated glomerulus are negligible. Glomerular σ is taken to be 1¹¹. One can therefore re-arrange the Starling equation to show that

$$L_p A = J_V / -\Delta\Pi \text{ (nl.min}^{-1}\text{.mmHg}^{-1}\text{)} \quad \text{(equation II)}$$

(where $\Delta\Pi$ is the difference between capillary and perfusate oncotic pressure)

In addition to the calculation of $L_p A$, the fold change in glomerular volume was calculated for all glomeruli exposed to the same experimental conditions, and at all timepoints between 0.1 seconds prior to, and at least 0.1 seconds after, the onset of glomerular shrinkage. A plot of fold change in glomerular volume versus time was thereby created (details are provided in Salmon et al⁹). A linear regression line applied to the initial period of mean glomerular shrinkage describes mean $J_V(f)$.

Endothelial cell glycosaminoglycan assay *in vitro*

Adult dermal human microvascular endothelial cells (Cambrex; 2nd passage) were grown in commercial media (EGM-2-MV) until 60-70% confluency. Serum-free media was introduced for 24 hours, followed by serum-free media \pm 200 ng.ml⁻¹ rhAng1 for 48 hours. Harvested supernatant was then centrifuged at 1000 rpm for 3 min to remove cellular debris, and incubated with 15 μ g.ml⁻¹ papain (P4762; Sigma, MO, USA) at 60°C for 60 minutes to eliminate interference from proteins and glycoproteins^{12,13}. Papain-treated supernatant was added to Alcian Blue solution at 1:4 dilution, the acidity of which (pH \approx 2) minimises interference from non-glycosaminoglycan molecules¹⁴. Absorbance of 488nm light was measured after 15 min incubation. The formation of complexes between glycosaminoglycans in the cell supernatant and Alcian Blue causes a reduction in absorbance. In keeping with previous reports, there was a linear relation between 488nm light absorbance and heparan sulphate mass (range 0.5 – 15 μ g: $r^2=0.86$). This relation was used to calculate the heparan sulphate mass equivalence of changes in 488nm light absorbance.

Supplementary figures

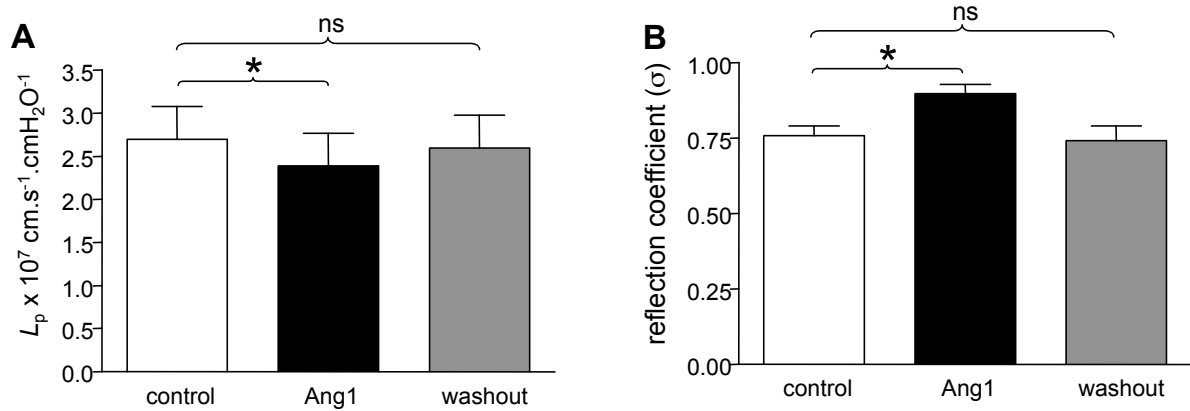


Figure I. The effects of angiopoietin-1 on L_p and $\sigma\Delta\pi$ are reversible. **A**, The reversibility of the effects of 30min perfusion with 200ng.ml^{-1} rhAng1 on L_p and σ were assessed by performing a further series of vessel occlusions after 35 minutes further perfusion with 30mg.ml^{-1} BSA alone. L_p fell in response to Ang1 (* $p < 0.05$ vs baseline (Friedman with Dunn's correction)), and returned to baseline values after washout (^{ns} $p > 0.05$ vs baseline (Friedman with Dunn's correction)). **B**, $\sigma\Delta\pi$ values rose in response to Ang1 perfusion, and again fell to baseline values following the washout perfusion period (repeated measures ANOVA for both $\sigma\Delta\pi$ and σ : overall $p < 0.001$; Bonferroni's correction - baseline vs rhAng1: * $p < 0.01$; baseline vs washout: ^{ns} $p > 0.05$). As for the effects of Ang1 on L_p , there was again no significant relation between baseline $\sigma\Delta\pi$ and the magnitude of change in $\sigma\Delta\pi$ elicited by Ang1 treatment (Pearson $r = -0.4$, $p > 0.25$, $n = 10$). In agreement with previous studies¹⁵, there was also no significant relation between baseline L_p and baseline σ (Spearman $r = 0.36$; $p > 0.15$; $n = 15$).

Supplementary discussion

We have been unable to examine the morphology and function of the endothelial glycocalyx in the single isolated (non-perfused) glomerular permeability assay directly for technical reasons. Specifically, this examination would require perfusion of individual glomeruli (both with pronase transiently, and with protein-free solution prior to glycocalyx staining of Alcian Blue). In addition, the confounding effects that pronase digestion may have on the glomerular basement membrane (which makes a significant contribution to the barrier properties of the glomerular capillary wall) would confound interpretation of these experiments. This latter situation contrasts with the situation in continuous microvascular beds such as the mesentery, in which endothelial cell structures alone (glycocalyx, intercellular cleft) dominate regulation of permeability coefficients.

We suggest that the depth of glycocalyx observed in our study (45nm under baseline conditions) is consistent with glycocalyx depths reported in the same microvascular network (31 – 100nm)¹⁶. The depth lies towards the lower end of the range of depths (20 – 1000nm) reported in studies of other vascular beds, possibly because of anatomical variations in endothelial glycocalyx composition¹⁷, and for methodological reasons (including depth measurement by electron microscopy rather than dextran exclusion or haematocrit assessment¹⁸, and absence of oxygen-carrying fixative¹⁹). The use of frog microvessels throughout this report permits these (and other: e.g. effects of pronase on L_p and glycocalyx²⁰) direct comparisons with the few previous studies of microvascular endothelial glycocalyx that exist in the literature. We confirmed that Ang1 also acts in a similar manner on mammalian microvessels by demonstrating identical effects of Ang1 on L_p in rat mesenteric microvessels.

Supplementary references

1. Hillman NJ, Whittles CE, Pocock TM, Williams B, Bates DO. Differential effects of vascular endothelial growth factor-C and placental growth factor-1 on the hydraulic conductivity of frog mesenteric capillaries. *J Vasc Res* 2001;**38**:176-186.
2. Glass CA, Harper SJ, Bates DO. The anti-angiogenic VEGF isoform VEGF165b transiently increases hydraulic conductivity, probably through VEGF receptor 1 in vivo. *J Physiol* 2006;**572**:243-257.
3. Gamble JR, Drew J, Trezise L, Underwood A, Parsons M, Kasminkas L, *et al.* Angiopoietin-1 is an antipermeability and anti-inflammatory agent in vitro and targets cell junctions. *Circulation Research* 2000;**87**:603-607.
4. Leach L, Sturgess H, Marsden J, The effect of Angiopoietin-1 on VEGF-induced leakage in human fetoplacental vessels, in *41st Meeting of the British Microcirculation Society*, Vol. 11, Microcirculation, University of Sheffield, UK, pp. 527-558 (2004).
5. Wann AK, Ingram KR, Coleman PJ, McHale N, Levick JR. Mechanosensitive hyaluronan secretion; stimulus-response curves & role of transcription-translation-translocation in rabbit joints. *Exp Physiol* 2009.
6. Adamson RH, Lenz JF, Zhang X, Adamson GN, Weinbaum S, Curry FE. Oncotic pressures opposing filtration across non-fenestrated rat microvessels. *J Physiol* 2004;**557**:889-907.
7. Kajimura M, Wiig H, Reed RK, Michel CC. Interstitial fluid pressure surrounding rat mesenteric venules during changes in fluid filtration. *Exp Physiol* 2001;**86**:33-38.
8. Michel CC, Phillips ME. Steady-state fluid filtration at different capillary pressures in perfused frog mesenteric capillaries. *J Physiol* 1987;**388**:421-435.
9. Salmon AH, Neal CR, Bates DO, Harper SJ. Vascular endothelial growth factor increases the ultrafiltration coefficient in isolated intact Wistar rat glomeruli. *J Physiol* 2006;**570**:141-156.
10. Savin VJ, Terreros DA. Filtration in single isolated mammalian glomeruli. *Kidney Int* 1981;**20**:188-197.
11. Savin VJ, Sharma R, Lovell HB, Welling DJ. Measurement of albumin reflection coefficient with isolated rat glomeruli. *J Am Soc Nephrol* 1992;**3**:1260-1269.
12. Farndale RW, Buttle DJ, Barrett AJ. Improved quantitation and discrimination of sulphated glycosaminoglycans by use of dimethylmethylene blue. *Biochim Biophys Acta* 1986;**883**:173-177.
13. Farndale RW, Sayers CA, Barrett AJ. A direct spectrophotometric microassay for sulfated glycosaminoglycans in cartilage cultures. *Connect Tissue Res* 1982;**9**:247-248.
14. Gold EW. The quantitative spectrophotometric estimation of total sulfated glycosaminoglycan levels. Formation of soluble alcian blue complexes. *Biochim Biophys Acta* 1981;**673**:408-415.
15. Michel CC. Filtration coefficients and osmotic reflexion coefficients of the walls of single frog mesenteric capillaries. *J Physiol* 1980;**309**:341-355.
16. Adamson RH, Clough G. Plasma proteins modify the endothelial cell glycocalyx of frog mesenteric microvessels. *J Physiol* 1992;**445**:473-486.
17. Henry CB, Duling BR. Permeation of the luminal capillary glycocalyx is determined by hyaluronan. *Am J Physiol* 1999;**277**:H508-514.
18. Pries AR, Secomb TW, Gaehtgens P. The endothelial surface layer. *Pflugers Arch* 2000;**440**:653-666.

19. Rostgaard J, Qvortrup K. Electron microscopic demonstrations of filamentous molecular sieve plugs in capillary fenestrae. *Microvasc Res* 1997;**53**:1-13.
20. Adamson RH. Permeability of frog mesenteric capillaries after partial pronase digestion of the endothelial glycocalyx. *J Physiol* 1990;**428**:1-13.